
# Oxygen influence in the magnetic and the transport properties of ferroelectric/ferromagnetic heterostructures

J. Gonzalez Sutter, L. Neñer, H. Navarro, G. Leyva, S. Fusil, K. Bouzehouane, N. Haberkorn, M. Sirena

PII: S0040-6090(17)30600-4
DOI: doi: 10.1016/j.tsf.2017.08.020
Reference: TSF 36162

To appear in: *Thin Solid Films*

Received date: 31 January 2017
Revised date: 7 August 2017
Accepted date: 11 August 2017

Please cite this article as: J. Gonzalez Sutter, L. Neñer, H. Navarro, G. Leyva, S. Fusil, K. Bouzehouane, N. Haberkorn, M. Sirena , Oxygen influence in the magnetic and the transport properties of ferroelectric/ferromagnetic heterostructures, *Thin Solid Films* (2017), doi: 10.1016/j.tsf.2017.08.020

# Oxygen influence in the magnetic and the transport properties of ferroelectric/ferromagnetic heterostructures.

J. Gonzalez Sutter[1,2], L. Neñer[1], H. Navarro[1,2], G. Leyva[3], S. Fusil[4], K. Bouzehouane[4], N. Haberkorn[1,2], and M. Sirena[1,2].

[1] Centro Atómico Bariloche, Instituto Balseiro – CNEA & Univ. Nac. de Cuyo, Av. Bustillo 9500, 8400 Bariloche, Rio Negro – Argentina.

[2] Consejo Nacional de Investigaciones Científicas y Técnicas, Centro Atómico Bariloche, Av. Bustillo 9500, 8400 Bariloche, Rio Negro - Argentina.

[3] Centro Atómico Constituyentes, 1650 San Martín, Buenos Aires, Argentina.

[4] Unite Mixte Physique CNRS/Thales, 1 Avenue Augustin Fresnel, 91767 Palaiseau, France.

Abstract.

Oxygen vacancies in oxides nanoestructures are the origin of many intriguing phenomena. We have studied the influence of the oxygen pressure in the tunneling properties of a ferroelectric barrier, $Ba_{0.25}Sr_{0.75}TiO_3$ (BSTO), grown over a ferromagnetic electrode. A phenomenological model description was used to obtain critical information about the structure and electrical properties of ultra thin BSTO layers using conductive atomic force microscopy. The BSTO layers present good insulation properties. Reducing the oxygen content increases the conductivity of the samples. The tunneling of the current carriers is probably the main conduction mechanism for samples with higher barrier thicknesses.

Keywords : CAFM, ultra-thin oxides, multiferroic nanostructures.

## I. Introduction.

Manganites compounds have been studied for many decades [1,2]. Nevertheless, a renewed interest in these systems took place in the early 90s. The origin of this interest was based essentially in two important properties of manganite systems: the colossal magneto-resistance effect [3] and the interplay between magnetic, transport and structural properties, which gives place to many intriguing phenomena. On the other hand, manganites and oxides with perovskite structure have become the key component in the development of an important number of devices, going from magnetic sensors, memory systems, new electronic devices, multiferroic tunnel junctions to field effect transistors. The possibility to tune the physical properties of these systems by different "extrinsic" effects like stress or chemical composition has given place to a novel area of study in basic physics and technological applications known as functionalized oxides and surface engineered systems (e. g. bilayer and multilayer nanostructures).

However, the growth and control of the physical properties of oxides could be difficult. In particular, the oxygenation of the samples is important since oxygen vacancies are a common defect in oxides nanostructures [4]. Usually a post deposition annealing processes is needed in order to achieve the correct stoichiometry. It is worth noticing that controlling and understanding the role of oxygen vacancies in the physical properties of oxides is critical since they are the origin of many fundamental and novel phenomena [4]. These phenomena include induced ferromagnetism [5,6], two dimensional electron gases in $LaAlO_3/SrTiO_3$ interfaces [7] and oxygen vacancies could contribute to the fatigue and aging effects in ferroelectric materials [4,8]. Additionally, this kind of defects are responsible of some interesting technological applications, such as memristors devices [9, 10]. Ferroeletric barriers has been used in the last years to induce additional resistance states in multiferroic tunnel junctions due to the interplay of the current flow and the polarization of the barrier which modifies the tunneling energy barrier [11].

The aim of this work is to study the oxygen influence in the physical properties of multiferroic heterostructures. There has been little experimental work done to understand the role of oxygen vacancies in the tunneling process across thin oxide barriers. In this context, it is particularly interesting the study of the electrical transport through a ferroelectric layer. Conductive atomic force microscopy (CAFM) has been used to study $La_{0.8}Ba_{0.2}MnO_3/Ba_{0.25}Sr_{0.75}TiO_3$ bilayes, using different oxygen pressures during the post deposition cooling of the samples. We have developed a phenomenological method and a

characterization analysis using CAFM that allows to study the transport and morphological properties of thin insulting layers over conducting electrodes [12]. This model was used to obtain critical information for the development of tunnel junctions like devices, i.e. information about the energy barrier, the attenuation length and the width of the barrier thickness distribution.

## II. Experimental Details.

$La_{0.8}Ba_{0.2}MnO_3$ (LBMO) and $Ba_{0.25}Sr_{0.75}TiO_3$ (BSTO) bilayers were grown on $SrTiO_3$ (100) single crystal substrates by DC and low power ($5000W/m^2$) RF magnetron sputtering, respectively. The substrate temperature was kept at 720°C in an argon (90 %) / oxygen (10 %) atmosphere at a pressure of 53 Pa for the whole sputtering process. We have deposited thin LBMO electrodes (30 ± 1 nm) in order to reduce the roughness of the surface, increasing the quality of the BSTO barrier as deduced from previous works [12]. BSTO layers of different thicknesses (*d*: 2, 4.5, and 7 nm) were deposited on top of the manganite electrode. After deposition, the samples were cooled down to room temperature at a rate of 6 °C/min under different oxygen pressures. One series of samples was cooled down using an oxygen pressure of 13330 Torr, while a second series of samples was cooled down using a reduced oxygen pressure of 667 Torr. We expect that lower oxygenation pressures decreases the oxygen content of the samples. The influence of the oxygen pressure on the magnetic properties of the samples was study using a using a commercial SQUID magnetometer. Low angle X-Ray reflectometry was used to obtain information about the surface and interface quality of the bilayers.

CAFM measurements were performed in a Dimension 3100 © Bruker microscope, using diamond doped conductive tips at room temperature. A complete characterization of the samples was made by analyzing the topographic and CAFM current information at different scale lengths. In order to increase reproducibility, the images were taken using the same deflection point (i.e. the same tip-surface pressure) and the same polarization voltage (typically 5.2 V). To avoid any surface charge or chemical alteration of the surface due to tip-sample interaction, all the images were taken in "virgin", previously untouched areas. Samples were measured within two or three days from the deposition date in order to reduce any possible passivation of the surface (significant changes in the transport properties were not observed until the samples were exposed for several days in air). In order to reduce dispersion and electrical noise, current-voltage (I(V)) responses of the samples were measured

at different surface spots (typically around 10). To assure the perfect condition of the tip, high resolution images of the samples were taken and compared to previous measured data, checking the sharpness of the images and the absence of any experimental artifacts.

## III. Results and discussion.

X-Ray diffraction patterns of the multiferroic bilayers show that the samples present a good crystalline growth, textured in the direction perpendicular to the substrate. The bilayers present good magnetic properties, independently of the oxygenation pressure during the cooling down of the samples. The ferromagnetic transition temperature (Tc) of the electrodes, obtained from magnetization measurements is around 245K and the coercive field of the samples is around 12 mT. Previous results indicate that oxygen vacancies in manganite films and bulk compounds lead to a decrease of the Curie temperature and an increase of the resistivity [13,14]. However, the influence of the oxygenation pressure during the cooling of the samples could be reduced, due to the presence of the BSTO layer. This layer could act as a diffusion barrier for the oxygen vacancies and no significant change on the magnetic properties of the samples could be observed for the two oxygen pressures used for the growth of the samples.

Figure 1 shows the topographic (left) and CAFM (right) images of the LBMO/BSTO bilayers for different thicknesses of the insulating layer. The corresponding images of a manganite film are also included for comparison purposes. In general, the samples present a low RMS roughness (~ 0.5 nm). The mean density of surface defects seems to be equivalent to the ones observed in similar systems [15,16], around 0.3 def/$\mu m^2$. The grow of thin oxides layers like manganite films and High Tc superconductors is complex and usually present and important presence of outgrowths or small surface defects. This kind of defects usually can be seen as pinholes or hot spots, in bilayers samples, due to their high conductance values, compared with the barrier. In general the density of defects varies from sample to sample (going from 0.1 def/$\mu m^2$ to more than 1 def/$\mu m^2$) and is probably related to the quality of the substrate surface. An extremely low density of surface defects could be obtained through a careful optimization and treatment of the substrate [17]. BSTO layers present very good insulating properties. The mean tunneling current decreases as the thickness of the insulating layer increases. CAFM images present an important distribution of the tunneling current, which is typical for these systems and it is generally ascribed to a distribution of the barrier

thickness [12,18,19]. CAFM measurements for the single manganite films and very low thickness of the barrier (i.e. 2 nm) were performed at lower polarization voltages due to the saturation of the CAFM sensor and the dielectric breakdown of the barrier. Reducing the oxygenation pressure during the cooling of the samples seems to increase the tunneling current through the ferroelectric barrier. This effect is almost unnoticeable for thin insulating barriers, but it becomes more important for thicker BTO layers (i.e. 7 nm) (Figure 2). In general, a more conducting behavior in bulk or thick films samples is observed when the oxygen content in the samples is changed. This effect is usually ascribed to ionic conductance or oxygen vacancies migration. However, this mechanism are in generally thermally activated and become dominant at very high temperatures (T>1000K) [20,21]. The conductivity due to the electronic and ionic transport becomes very small at room temperature and the tunneling of the carriers is expected to become dominant, for thin insulating layers. In this context, the increasing CAFM current with decreasing oxygen pressure during the post-deposition annealing, could be related to a reduction of the energy gap or the barrier energy.

The dispersion in the CAFM current can be generally ascribed to a barrier thickness distribution. If tunneling is the main transport mechanism in these samples, the Gaussian distribution of the barrier thickness gives place to a lognormal current distribution, due to the exponential dependence of the tunneling current with the barrier thickness [19,22]. Figure 3 shows the CAFM current distributions for the LBMO/BSTO bilayers with different insulating layer thicknesses and two different oxygen pressures. The lognormal distribution seems to fit well the experimental data obtained from the CAFM images, consistently with the tunneling process of the carriers through the insulating barrier. As the thickness of the barrier increases the current distribution shifts to lower values, as expected. The CAFM current distributions present similar distribution widths, for the two oxygenation conditions. The dispersion corresponds to a thickness distribution width of 0.6 nm, in good agreement with the measured roughness values. This value is similar than one obtained from the fitting of the low angle X-Ray diffraction spectra and is consistent with the values obtained in oxides multilayers systems grown by sputtering, due to the growth mechanism and inter diffusion of the layers.

Outgrowths and surface defects in the samples present important height gradients that break the insulating layer given place to high conductance spots (observed as peaks in the current distribution at the saturation value of the CAFM sensor). The increase of the CAFM current for the 7 nm BSTO barrier and lower oxygenation pressure can be clearly seen in the figure. The conductance of the ferroelectric layer increases almost one order of magnitude for a reduced oxygen pressure of 667 Pa.

Rowell et. al. developed a set of criteria to distinguish tunneling from other transport mechanisms in the superconducting junctions [23]. Three of these criteria continue to apply in our system: the exponential thickness dependence of the current, the parabolic shape of the differential conductance as a function of voltage, and a weak insulating-like temperature dependence of the conductance (or resistance). We have verified the first two criteria in our systems (Figure 4 and Figure 5). However, the group of Professor Ivan K. Schuller have demonstrated that the only reliable criterion to rule out the presence of pinholes in tunneling junctions is the temperature dependence of the resistance [24]. Nevertheless, it should be notice that if pinholes are present in the barrier they should be smaller than the conductive AFM tip radius (~100nm) and its density should be reduced exponentially with increasing barrier thickness. Even if we cannot totally rule out the presence of pinholes in the insulting barrier, its influence should be greatly reduced for the samples with higher barrier thicknesses (d>4nm).

Assuming a tunneling conduction mechanism, the decay of the tunneling current as function of the barrier thickness would allow to estimate the attenuation length ($\lambda$) for the different oxygenation pressures. We have found that $\lambda$ is around 0.3 nm for the samples that were cooled down using an oxygenation pressure of 13300 Pa. The samples that were cooled with a lower oxygen pressure present a higher attenuation length ($\lambda^{5\ \mathrm{Torr}} \sim 0.4$ nm) consistent with the more "conducting" behavior. These values are equivalent to the ones observed previously for similar systems [12]. The barrier energy can be estimated considering a rectangular barrier shape, for different applied voltages. Under this assumptions, in the Simmons's model [25], the barrier energy is given by $\phi = \left[\frac{3he}{8\pi\sqrt{2m^*}}\frac{V}{\lambda}\right]^{2/3}$ where $h$ is the Planck's constant, $m^*$ is the effective mass of the charge carriers, $e$ is the electron charge and $V$ is the applied voltage. $m^*$ is given by the band structure of BSTO, and for the present calculations it has been consider that $m^*=m_e$ as suggested by ARPES measurements of the band structure for similar conducting manganites [26,27] . We have found that $\phi^{13330\mathrm{Pa}} \sim 0.7$ eV and $\phi^{667\mathrm{Pa}} \sim 0.6$ eV. These values are coherent with the ones observed for a thin $BaTiO_3$ barrier, grown over a HightTc superconductor electrode [28]. It should be noticed that increasing the density of pinholes would result in a reduction of the effective "barrier height" obtained with this method. In this way, high values of the insulting barrier height are consistent with a small influence of pinholes in the electronic transport of the sample.

The typical I(V) curves corresponding to the LBMO/BSTO bilayers, with different insulating thicknesses and for the two oxygen pressures are shown in Figure 6. The LBMO electrode presents a non-linear behavior of the current voltage characteristics; this is usually the case for oxide electrodes due to the passivation of the surface exposed to the air. The experimental data are fitted using a phenomenological model [12]: $Ln(I(V,d)) = A_0(d) + \alpha(d).Ln(V)$ It can be shown that this dependence leads to $I(V,d) = I_0 V^{\alpha_0} e^{-\frac{d}{\lambda}}$, where λ is the attenuation length of the charge carriers in the barrier. This is coherent with the tunneling of the transport carriers across an insulating barrier [25]. Short attenuation lengths indicate an extremely fast decay of the tunnelling current, corresponding to high insulating barriers. The measured current voltage response of the samples presents the same behavior than the CAFM images. The tunneling current rapidly decreases for increasing barrier thicknesses. Additionally, the samples that were cooled down with a reduced oxygen pressure present a higher current flowing through the barrier. It is important to notice that the conduction mechanism in both series of samples seems to be the same. The presence of very small pinholes in the barrier can be not totally rule out in our system. However, the log-normal CAFM current distribution, the exponential increase of the resistance with increasing barrier thicknesses and the voltage dependence of the conductance are coherent with the tunneling of the current carries through the oxide layer.

## IV. Conclusions.

We have studied the influence of the oxygen pressure in the tunneling properties of a ferroelectric barrier grown on top of a ferromagnetic electrode. A phenomenological approach was used to obtain critical information about the structure and electrical properties of ultra-thin $Ba_{0.25}Sr_{0.75}TiO_3$ (BSTO) layers, grown over a ferromagnetic electrode, using conductive atomic force microscopy. The tunneling of the current carriers is probably the main conduction mechanism for samples with higher barrier thicknesses. The short attenuation lengths and the high energy barriers obtained for the ferroelectric layers indicate the good insulation properties of the samples. We have found that reducing the oxygen content increases the tunneling current due to a decrease of the energy barrier. It should be notice that no change of the conduction mechanism was observed for the different oxygenation conditions.

.

The authors would like to thank R. Benavides for his extraordinary technical support and Drs. J. Guimpel and Dr. H. Pastoriza for the use of the micro and nanofabrication facilities. Dr. A. Butera contributed to the critical reading of the manuscript. This work was partially supported by the ANPCYT (PICT-2014-2237). MS and JG acknowledge the financial support from the international cooperation programs PICS level 2 CNRS/CONICET and the PEOPLE MARIE CURIE ACTIONS, International Research Staff Exchange Scheme, Call: FP7-PEOPLE-2012-IRSES, COEF-magNANO.

[1] G. H. Jonker and J. H. Van Santen, Ferromagnetic compounds of manganese with perovskite structure, Physica **16**, (1950), 337.

[2] C. Zener, Interaction between the d-Shells in the Transition Metals. II. Ferromagnetic Compounds of Manganese with Perovskite Structure, Physical Review **82**, (1951), 403

[3] S. Jin, T. H. Tiefel, M. McCormack, R. A. Fastnacht, R. Ramesh and L. H. Chen, Thousandfold Change in Resistivity in Magnetoresistive La-Ca-Mn-O Films, Science **264**, (1994), 413.

[4] Menglei Li, Jia Li, Long-Qing Chen, Bing-Lin Gu and Wenhui Duan, Effects of strain and oxygen vacancies on the ferroelectric and antiferrodistortive distortions in PbTiO3/SrTiO3 superlattice, Physical Review B, **92**, (2015), 115435.

[5] G. S. Chang, J. Forrest, E. Z. Kurmaev, A. N. Morozovska, M. D. Glinchuk, J. A. McLeod, A. Moewes, T. P. Surkova, and Nguyen Hoa Hong, Oxygen-vacancy-induced ferromagnetism in undoped SnO2 thin films, Phys. Rev. B **85**, (2012), 165319.

[6] Peng Zhan, Weipeng Wang, Can Liu, Yang Hu, Zhengcao Li, Zhengjun Zhang, Peng Zhang, Baoy Wang and Xingzhong Cao, Oxygen vacancy-induced ferromagnetism in un-doped ZnO thin films, Journal of Applied Physics, **111**, (2012), 033501.

[7] A. Ohtomo and H. Y. Hwang, A high-mobility electron gas at the LaAlO3/SrTiO3 heterointerface, Nature **427**, (2004), 423.

[8] C. H. Park and D. J. Chadi, Microscopic study of oxygen-vacancy defects in ferroelectric perovskites, Physical Review B, **57,** (1998), R13961.

[9] Strukov, D. B.; Snider, G. S.; Stewart, D. R.; Williams, S. R. (2008), The missing memristor found, Nature **453,** (2008), 7191

[10] A. Beck, J. G. Bednorz, Ch. Gerber, C. Rossel and D. Widmer, Reproducible switching effect in thin oxide films for memory applications, Applied Physics Letters **77**, (2000), 139

[11] M. Ye. Zhuravlev, R. F. Sabirianov, S. S. Jaswal, and E. Y. Tsymbal, Giant Electroresistance in Ferroelectric Tunnel Junctions, Physical Review Letter, **94**, (2005), 246802.

[12] M. Sirena, Roughness influence in the barrier quality of ferroelectric/ferromagnetic tunnel junctions, model, and experiments, Journal of Applied Physics, 110, (2011), 063923.

[13] V.G. Prokhorov, G. G. Kaminsky, V. A. Komashko, Y. P. Lee, J. S. Park, H. C. Ri, Oxygen-deficiency-activated phase transition in a long-aged $La_{0.8}Ca_{0.2}MnO_3$ film, Applied Physics Letters, 80, (2002), 2707.

[14] W. Zhang, W. Boyd, M. Elliot, and W. Herrenden-Harkerand, The effects of oxygen content on the magnetoresistive behavior in La-Ca-Mn-O films grown on Si, Applied Physics Letters 69, (1996), 3929.

[15] M. P. Singh, W. Prellier, L. Mechin, C. H. Simon, and B. Raveau, Correlation between structure and properties in multiferroic La0.7Ca0.3MnO3/BaTiO3
superlattices, Journal of Applied Physics, **99**, (2006), 024105.

[16] M. Sirena, E. Kaul, M. B. Pedreros, C. A. Rodriguez, J. Guimpel, and L. B. Steren, Structural, magnetic and electrical properties of ferromagnetic/ferroelectric multilayers, Journal of Applied Physics, **109**, (2011), 123920.

[17] M. Sirena, L. Avilés Félix and N. Haberkorn, High transition temperature superconductor/insulator bilayers for the development of ultra-fast electronics, Applied Physics Letters, **103**, (2013), 052902.

[18] T. Fix, V. Da Costa, C. Ulhaq-Bouillet, S. Colis, A. Dinia; K. Bouzehouane and A. Barthélémy; High quality SrTiO3 tunnel barrier obtained by pulsed laser deposition, Applied Physics Letters, **91**, (2007), 083104.

[19] F. Bardou; Rare events in quantum tunneling, Europhysics Letters, **39**, (1997), 239.

[20] U. Balachandran and N. G. EROR, Electrical Conductivity in Strontium Titanate, Journal of Solid State Chemestry 39, (1981), 351.

[21] Christian Ohly, Susanne Hoffmann-Eifert, and Xin Guo, Jürgen Schubert, Rainer Waser, Electrical Conductivity of Epitaxial SrTiO3 Thin Films as a Function of Oxygen Partial Pressure and Temperature, Journal American Ceramic Society **89** (2006), 2845.

[22] V. Da Costa, M. Romeo, and F. Bardou, Statistical properties of currents flowing through tunnel junctions, Journal of Magnetism and Magnetic Materials, **258–259**, (2003), 90.

[23] J. M. Rowell, in Tunneling Phenomena in Solids, edited by E. Burstein and S. Lundqvist (Plenum, New York, 1969), p. 273.

[24] Johan J., Akerman, R. Escudero, C. Leighton, S. Kim, D.A. Rabson, Renu Whig Dave, J.M. Slaughter, Ivan K. Schuller, Criteria for ferromagnetic–insulator–ferromagnetic tunneling, Journal of Magnetism and Magnetic Materials 240 (2002) 86

[25] J. G. Simmons; Generalized Formula for the Electric Tunnel Effect between Similar Electrodes Separated by a Thin Insulating Film, Journal of Applied Physics, **34**, (1963), 1793.

[26] Peng Xu, T.J. Huffman, N.C. Branagan, M.M. Qazilbash, P. Srivastava, T. Goehringer, G. Yong, V. Smolyaninova & R. Kolagani, Novel aspects of charge and lattice dynamics in the hole-doped manganite La0.67Sr0.33MnO3, Philosophical Magazine, **95**, (2015), 2078.

[27] A. Chikamatsu, H. Wadati, H. Kumigashira, M. Oshima,1 A. Fujimori, M. Lippmaa, K. Ono, M. Kawasaki, and H. Koinuma, Gradual disappearance of the Fermi surface near the metal-insulator transition in La1−xSrxMnO3 thin films, Physical Review B, **76**, , (2007), 201103(R).

[28] H. Navarro, Ilkyu Yang, M. Sirena, Jeehoon Kim, and N. Haberkorn, Characterization of the insulator barrier and the superconducting transition temperature in GdBa2Cu3O7-d / BaTiO3 bilayers for application in tunnel junctions, Journal of Applied Physics, 118, (2015), 45308.

**Figure 1:** Topographic (lef) and CAFM (right) 6 μm x 6 μm images of $La_{0.8}Ba_{0.2}MnO_3$ and $Ba_{0.25}Sr_{0.75}TiO_3$ bilayers grown over $SrTiO_3$ with different BSTO thickness (2 nm (a), 4.5 nm (b) and 7 nm (c)). Shown for two different oxygen pressures used during the post-deposition cooling of the samples, 667 Pa (1) and 13330 Pa (2). The topographic and CAFM images of a manganite electrode are included on top for comparison.

**Figure 2:** Topographic (lef) and CAFM (right) 6 μm x 6 μm images of $La_{0.8}Ba_{0.2}MnO_3/Ba_{0.25}Sr_{0.75}TiO_3$ bilayers with a BSTO thickness of 7 nm and different oxygen pressures, 667 Pa (a) and 13330 Pa (b). Measurements were performed using a high sensitivity range (10pA/V).

**Figure 3:** Current distributions measured with a polarization voltage of 5.2 V, for LBMO/BSTO bilayers with different BSTO thicknesses and different oxygenation pressures, 667 Pa (a) and 13330 Pa (b). The lines correspond to the fittings using a log-normal distribution.

**Figure 4:** Conductance vs. applied voltage for LBMO/BSTO bilayers with different BSTO thicknesses and different oxygenation pressures, 667 Pa (open symbols) and 13330 Pa (close symbols).

**Figure 5:** Resistance as function of the barrier thickness, for LBMO/BSTO bilayers with different oxygenation pressures, 667 Pa (open symbols) and 13330 Pa (close symbols). The lines correspond to the linear fitting of the experimental data.

**Figure 6:** CAFM I(V) curves for the ferromagnetic/ferroelectric bilayers grown using different oxygen pressures during the cooling of samples. The solid lines are a linear fits of the experimental data ($Log(I) = A_0 + \alpha \, . \, Log(V)$). The inset shows $A_0$ and $\alpha$ as function of the barrier thickness ($d$), for the two series of samples. Open symbols correspond to an oxygen pressure of 667 Pa and close symbols correspond to an oxygen pressure of 13330 Pa.

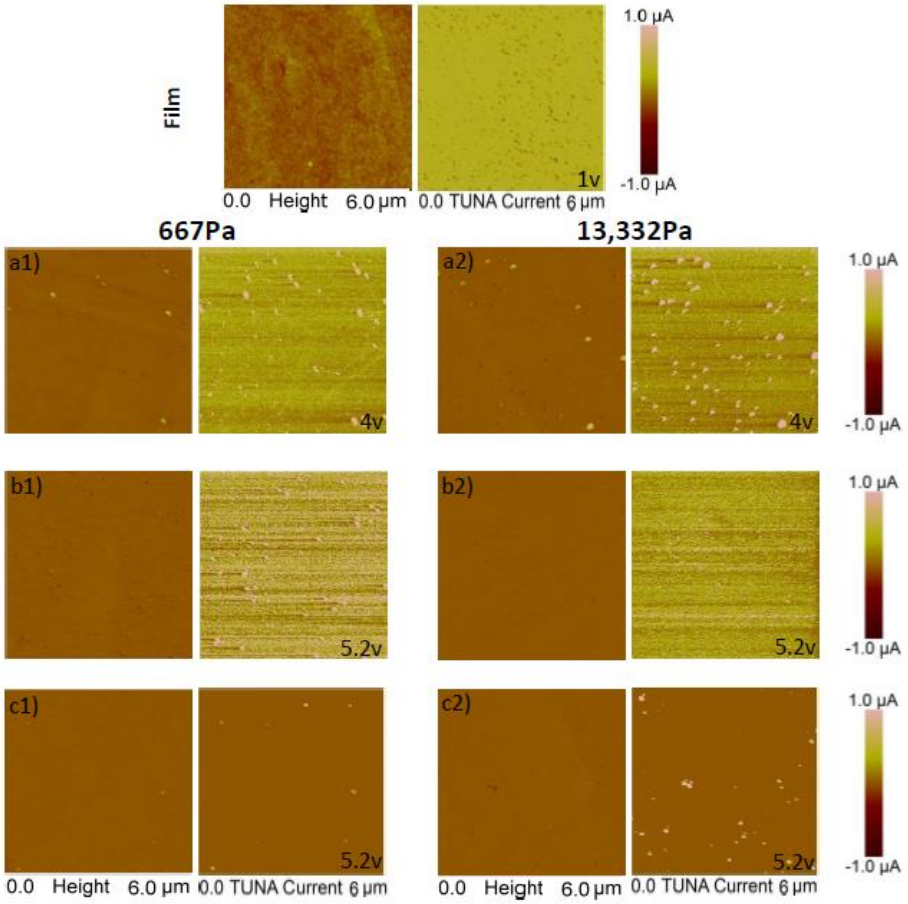


Fig. 1

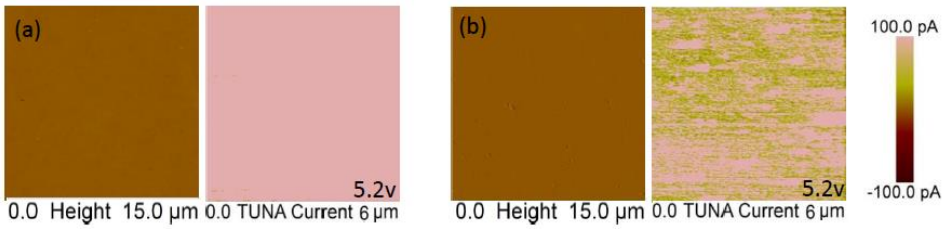


Fig. 2

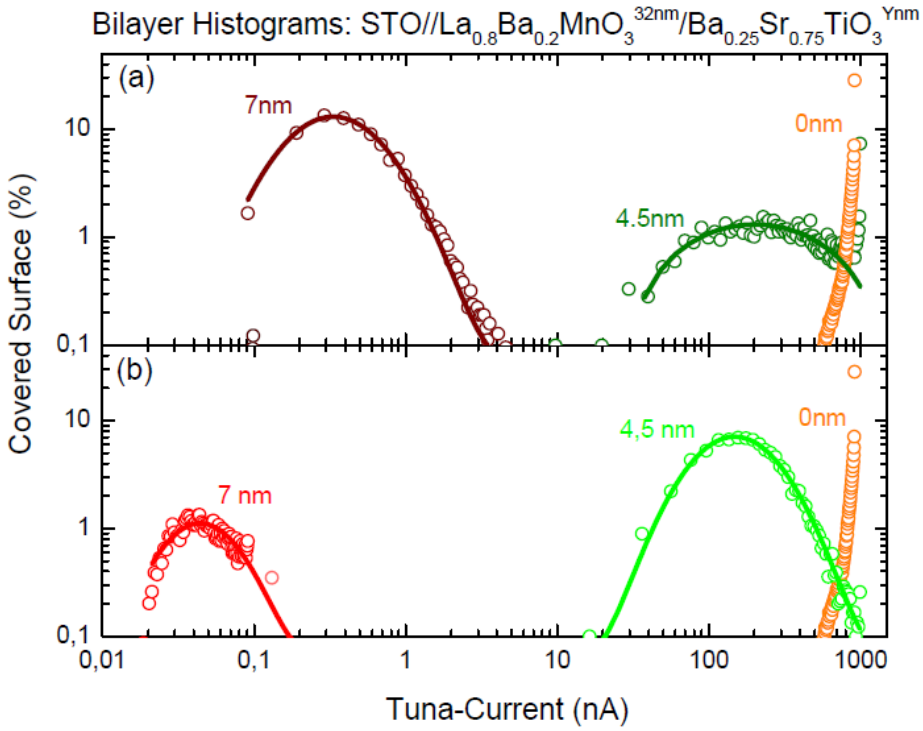


Fig. 3

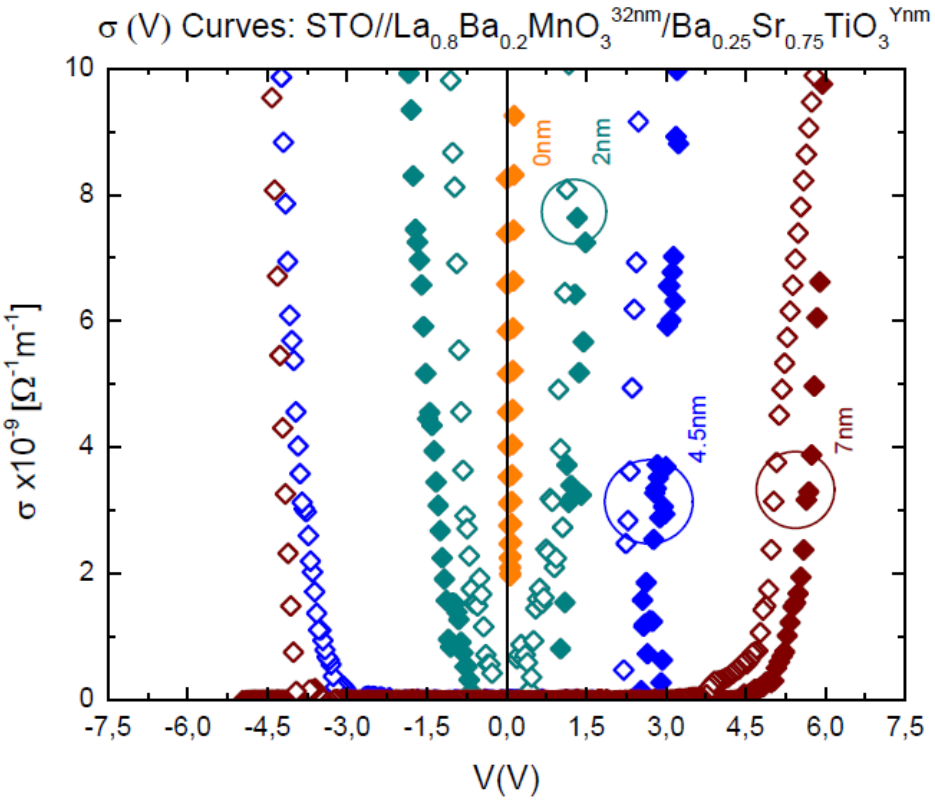


Fig. 4

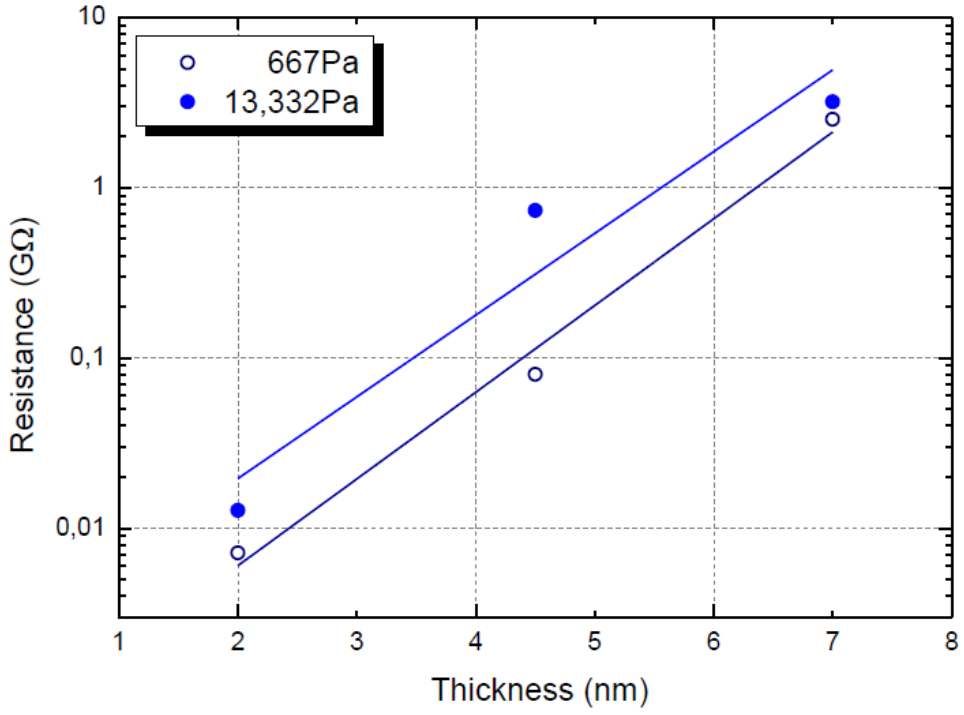


Fig. 5

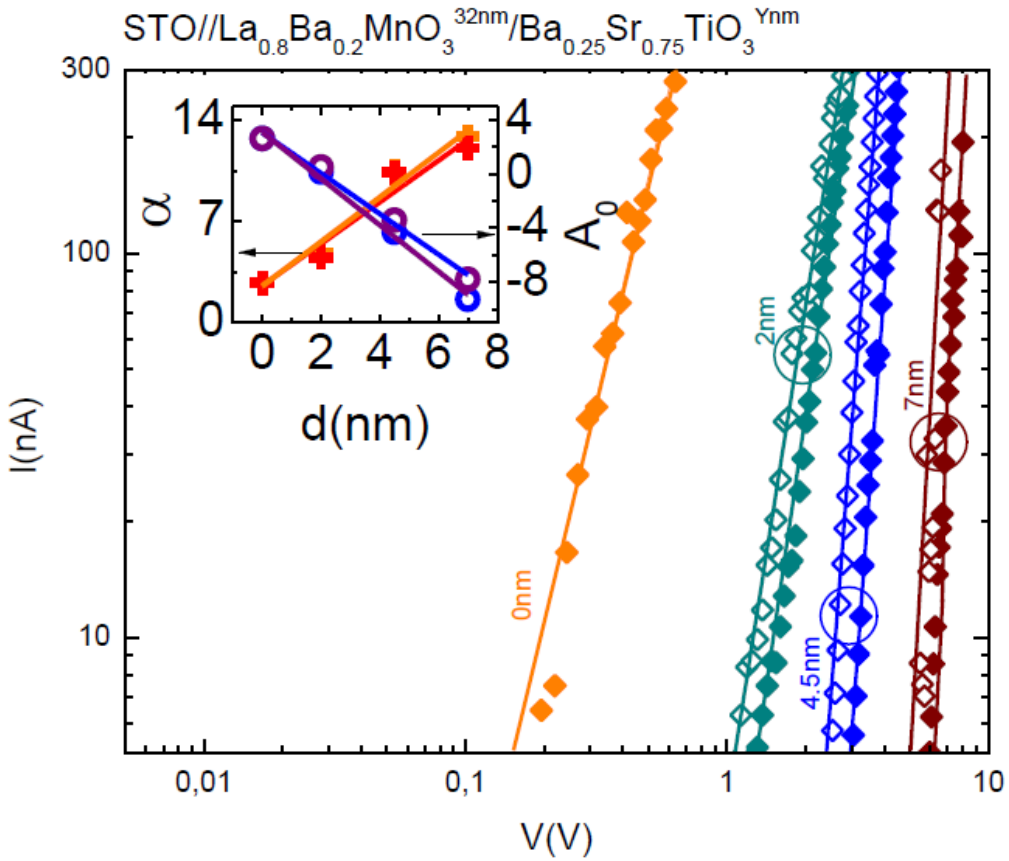


Fig. 6

**Highlights.**

- Oxygen vacancies increase the conductivity of the barrier
- The tunneling of the current carriers seems to be the main conduction mechanism.
- Oxygen vacancies decrease the energy barrier and increase the attenuation legth.